ACS APPLIED MATERIALS & INTERFACES

Research Article

www.acsami.org

Facile Method toward Hierarchical Fullerene Architectures with Enhanced Hydrophobicity and Photoluminescence

Shushu Zheng, Meilin Xu, and Xing Lu*

State Key Laboratory of Materials Processing and Die & Mold Technology, School of Materials Science and Engineering, Huazhong University of Science and Technology (HUST), Wuhan 430074, P. R. China

Supporting Information

ABSTRACT: A two-step self-assembly strategy has been developed for the preparation of fullerene hierarchical architectures. Typically, the precipitation method is utilized to synthesize the initial fullerene microstructures, and subsequently a drop-drying process is employed to facilitate the fullerene microstructures to self-assemble into the final hierarchical structures. Overall, this methodology is quite simple and feasible, which can be applied to prepare fullerene hierarchical structures with different morphological features, simply by choosing proper solvent. Moreover, the as-obtained C_{70} hierarchical structures have many superior properties over the original C_{70} microrods such as superhydrophobicity and unique photoluminescence behaviors, promising their applications as waterproof optoelectronics.

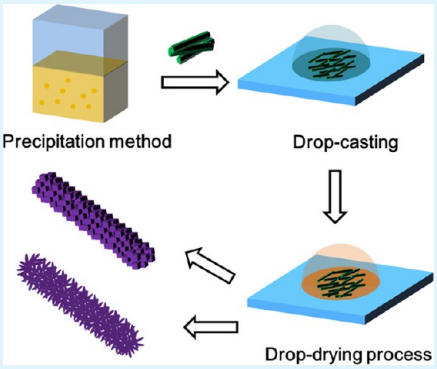

KEYWORDS: *fullerene, self-assembly, hierarchical structure, hydrophobicity, photoluminescence enhancement*

INTRODUCTION

Fullerenes have gathered much attention in materials science owing to their extensive potential applications in semiconductors, optoelectrical devices, and energy storage.[1−5] Following this trend, it is of great importance to ensure that fullerene molecules assemble into geometrically well-defined structures, and therefore function remains unexplored.[6−10] Fortunately, efficient synthetic routes developed for the fabrication of low-dimensional organic crystals composed of highly conjugated molecules provide opportunities for building of fullerene nano/microstructures.[11,12] Until now, fullerene molecules are readily crystallized to well-ordered one-dimensional (1D) or two-dimensional (2D) forms by self-assembly at liquid−liquid,[13−15] liquid−air,[16,17] or liquid−air−solid interfaces.[18−20] However, these approaches are always accompanied by the drawbacks of limited shape and dimensionality modulation, especially for the fabrication of complex structures. Moreover, effective and feasible nanostructuring is still lacking when compared to the profusely nanostructured inorganic materials.[21,22]

Over the past decades, hierarchical structures have always been a topic under intensive investigation in a variety of fields because of their promising applications in functional materials. Benefiting from the two or more structural levels, hierarchical structures have exhibited distinctive properties in electrochemistry,[23] photoelectrochemistry,[24] hydrophobicity,[25,26] and so on. Therefore, the introduction of hierarchical structures to fullerene crystals can of course be helpful for the full realization of their applications in various fields and bring new prospects for the development of fullerene nano/microstructures. Previous studies have revealed that C_{60} and single-walled carbon nanotubes, amphiphilic C_{60} derivatives, and C_{60}-porphyrin cocrystals can successfully self-assemble to hierarchical architectures in a controlled fashion.[27−30] However, controllable fabrication of fullerene hierarchical structures without functionalization or participation of other cocrystal molecules is still a challenging task.

Although one-step assembly routes such as liquid−liquid interfacial precipitation (LLIP) method[8,31−34] and drop-drying process[18,35,36] have shown great success in preparing well-defined 1D or 2D fullerene crystals, it is still demanding to develop a universal method to prepare fullerene hierarchical structures in a controllable manner. Herein, we propose a solution-driven self-assembly approach for the fabrication of fullerene hierarchical architectures (Figure 1). In detail, fullerene microstructures were first obtained from the liquid−liquid interface. Then a drop-drying method was employed for the reconstruction of the microstructures into different hierarchical structures. Our results show that the solvents applied in the drop-drying process are intercalated into the C_{70} crystals, and consequently they play a critical role in determining the morphology and crystalline structure of the final hierarchical architectures. Furthermore, the mechanism for the formation of hierarchical structures is systematically studied, and different morphologies based on C_{60} or C_{70} are readily obtained simply by alternating the solvents, showing the

Received: June 30, 2015
Accepted: August 31, 2015
Published: August 31, 2015

© 2015 American Chemical Society

DOI: 10.1021/acsami.5b05869
ACS Appl. Mater. Interfaces 2015, 7, 20285−20291

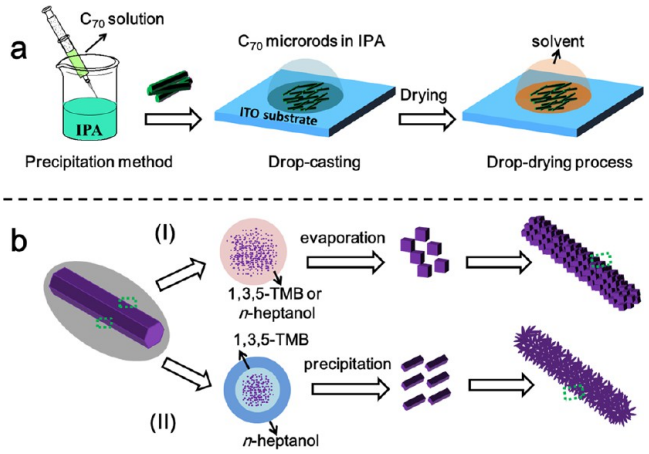

Figure 1. (a) Schematic illustration for the fabrication of C_{70} hierarchical architectures. (b) Schematic illustration for the formation mechanism of C_{70} hierarchical architectures when (I) TMB or *n*-heptanol or (II) the mixture of TMB and *n*-heptanol (*v*/*v* = 1/2) is used in the drop-drying process.

feasibility of this method. Finally, as a proof of concept, the properties of fullerene hierarchical structures are investigated. The second-level architecture brings enhanced hydrophobicity, even superhydrophobicity, to C_{70} crystals, also distinguishing photoluminescence behaviors in contrast with the original samples, revealing their potential applications for waterproof optoelectronics.

RESULTS AND DISCUSSION

In our experiment, fullerene hierarchical nanostructures were prepared by two steps, as illustrated in Figure 1a. Typically, C_{70} microrods (**C70−P**) were prepared by the precipitation method.[37] The precipitates (C_{70} microrods) were centrifugally separated from the suspension and washed with isopropyl alcohol (IPA) several times prior to vacuum drying. The SEM images of the as-prepared C_{70} microrods are displayed in Figure 2a. Then these C_{70} microrods were dispersed in IPA (40 mg/mL), and a uniform C_{70} film (about 12 mm^2) was formed by drop-casting the dispersion onto an ITO glass. Finally, 2 μL of appropriate solvent was dropped onto the dried film which was then kept at 25 °C for the drop-drying process. Here three kinds of solvents were employed in the drop-drying process: 1,3,5-trimethylbenzene (TMB), *n*-heptanol, and the mixture of TMB and *n*-heptanol (*v*/*v* = 1/2), and the obtained products are designated as **C70−P−TMB**, **C70−P−HA**, **C70−P−TMB/HA**, respectively.

Figure 2b−d displays the representative morphologies of the resulting hierarchical structures obtained from our method. Evidently, after the drop-drying process, the C_{70} microrods all evolve to well-defined hierarchical architectures. The morphological features of these three samples are remarkably different from each other in spite of the fact that they all retain the rodlike structures of the precursor (Figure 2b1−d1). In detail, small cubes (Figure 2b2 and 2c2) are generated on the surfaces with the average sizes of 0.5 and 1.0 μm when TMB and *n*-heptanol are used as solvents, respectively. Thus, we conclude that not only the good solvent (aromatic solvent)[38] but also the traditionally recognized poor solvent (alcohol)[38] can trigger the self-assembly process. In contrast, for **C70−P−TMB/HA**, it can be observed that nanorods with diameters of about 150−350 nm are formed on the surfaces (Figure 2d). Accordingly, the solvents utilized in the drop-drying process play a crucial role in the second-level morphology control of the as-obtained hierarchical structures.

The structures and compositions of original C_{70} microrods and the final C_{70} hierarchical structures were further characterized by a collection of experimental methods. The FTIR and Raman spectra of **C70−P** and C_{70} hierarchical structures (Figure S1) show the characteristic features of C_{70} molecules in all samples.[39] Figure 3a shows the corresponding

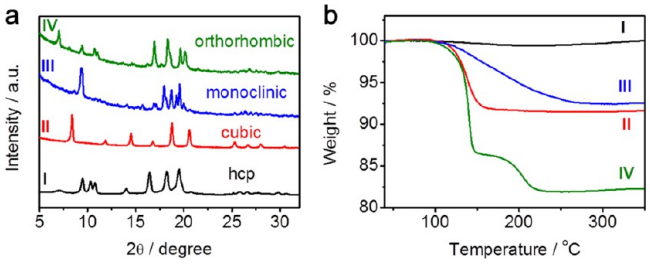

Figure 3. (a) XRD patterns and (b) TGA results of (I) **C70−P** and C_{70} hierarchical structures (II) **C70−P−TMB**, (III) **C70−P−HA**, and (IV) **C70−P−TMB/HA**.

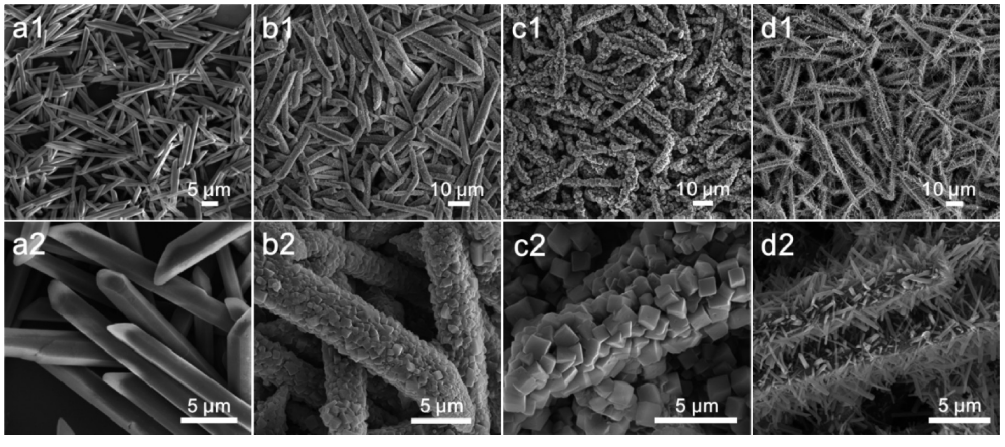

Figure 2. SEM images of (a) C_{70} microrods (**C70−P**) and (b−d) C_{70} hierarchical structures: (b) **C70−P−TMB**, (c) **C70−P−HA**, and (d) **C70−P−TMB/HA**.

DOI: 10.1021/acsami.5b05869
ACS Appl. Mater. Interfaces 2015, 7, 20285−20291

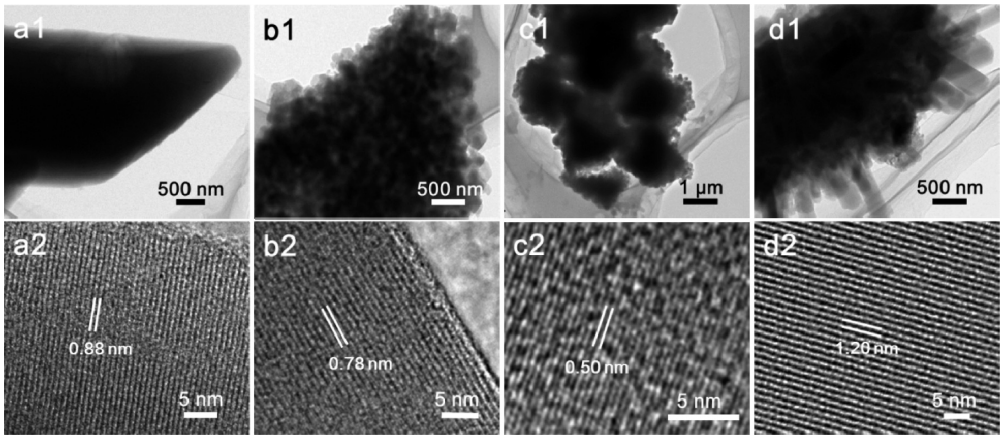

Figure 4. TEM (a1–d1) and HRTEM (a2–d2) images of (a) **C70–P** and the C_{70} hierarchical structures (b) **C70–P–TMB**, (c) **C70–P–HA**, and (d) **C70–P-TMB/HA**.

XRD patterns, which reveal that these treated samples have completely different crystalline types from the original C_{70} microrods. In detail, the original C_{70} microrods possess an hcp packing mode.[40] However, after the drop-drying process, the hcp phase transfers to cubic,[14] monoclinic,[41] and orthorhombic phases[42] for **C70–P–TMB**, **C70–P–HA**, and **C70–P–TMB/HA**, respectively, and the structural characteristics of each crystalline phase are shown in Table S1. According to the previous studies,[14,37] we speculate that the crystalline differences of C_{70} hierarchical structures are caused by the incorporation of different solvents in the crystals. All these three samples transfer to mixtures of hcp and fcc phases after 400 °C treatment at Ar atmosphere (Figure S4) because of the escaping of trapped solvents.[41] Furthermore, NMR and TGA measurements were conducted to confirm our speculation. The NMR results (Figure S3) and the weight loss processes from the TG results (Figure 3b) together clearly indicate that the solvents are successfully intercalated into C_{70} crystals for all the three C_{70} hierarchical structures. **C70–P–TMB** has a weight loss of 7.62% at a temperature range from 121 to 152 °C, due to the removal of TMB solvents. Similarly, **C70–P–HA** loses its 6.66% weight from 100 to 237 °C, which is assigned to the removal of *n*-heptanol. **C70–P–TMB/HA** has two weight loss processes with a total weight loss of 17.52%, demonstrating the entrapment of both TMB and *n*-heptanol molecules, which is also corroborated by the DTG results (Figure S2).

Transmission electron microscopy (TEM) results provide further insights into the morphological and structural features of the C_{70} hierarchical structures (Figure 4). It is clearly observed that all these rodlike assemblies consist of numerous primary C_{70} nanocubes or nanorods (Figure 4b1–d1). Furthermore, it is noteworthy that not only does the surface of the microrods undergo the reconstruction but also the whole microrods participate in the second-step self-assembly process. Moreover, our conclusion is also supported by XRD results (Figure 3a), which clearly show that no hcp phase of the original C_{70} microrods is retained in the final products. As demonstrated in Figure 4a2, the original C_{70} microrods are single crystals with a lattice distance of 0.88 nm. After the drop-drying process, the continuous lattice fringes in HRTEM images are observed in every single nanocube or nanorod of the C_{70} hierarchical structures, indicating that the resulting C_{70} hierarchical structures are also composed of single-crystal units. In addition, the lattice values are in good agreement with the XRD results above. As shown in Figure 4b2, the distance between two adjacent planes is 0.78 nm, very close to $d(011)$ of the cubic lattice. The respective lattice distances in Figure 4c2 and Figure 4d2 are 0.50 and 1.20 nm, which can be assigned to the (200) plane of the monoclinic structure and the (003) plane of the orthorhombic structure, respectively. On the basis of these experimental findings, the reorganization in the second step is assured to be a thorough self-assembly process, not only occurring at the surfaces of C_{70} microrods.

To study the formation mechanism of the hierarchical structures, one-step drop-drying experiments (based on C_{70}/TMB or C_{70}/*n*-heptanol) and precipitation experiment (based on C_{70}/TMB/*n*-heptanol) were conducted. The products obtained from C_{70}/TMB, C_{70}/*n*-heptanol, and C_{70}/TMB/*n*-heptanol are denoted as **C70–TMB**, **C70–HA**, and **C70–TMB/HA**, respectively. As displayed in Figure 5, C_{70} cubes are obtained from drop-drying of both C_{70}/TMB and C_{70}/*n*-heptanol solutions. However, C_{70} nanorods are formed at the

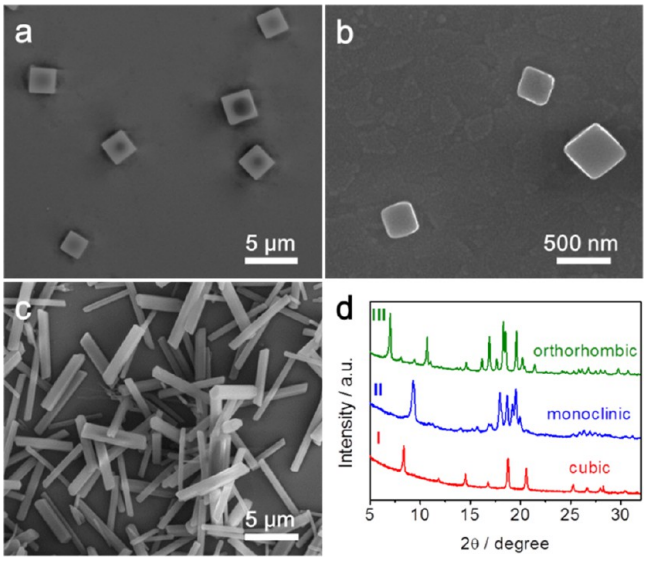

Figure 5. SEM images of C_{70} nanostructures prepared from one-step drop-drying process or precipitation method: (a) **C70–TMB**, (b) **C70–HA**, and (c) **C70–TMB/HA**. (d) XRD patterns of the as-mentioned C_{70} nanostructures (I) **C70–TMB**, (II) **C70–HA**, and (III) **C70–TMB/HA**.

DOI: 10.1021/acsami.5b05869
ACS Appl. Mater. Interfaces 2015, 7, 20285–20291

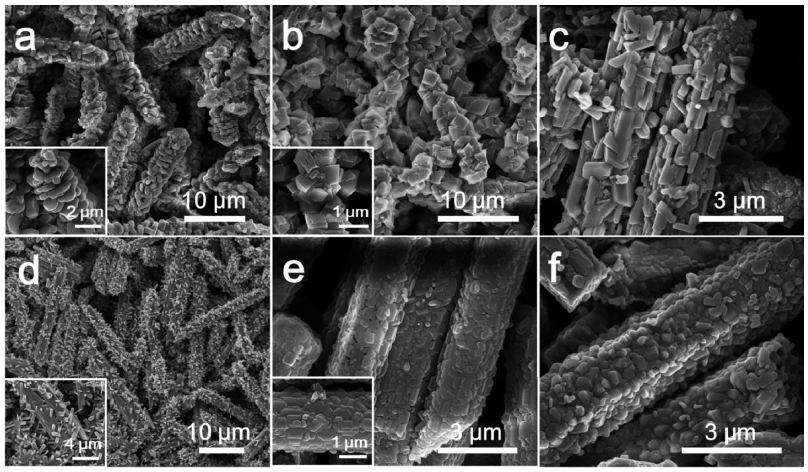

Figure 6. SEM images of C_{70} hierarchical structures prepared from C_{70} microrods when different solvent mixtures were applied in the drop-drying process: (a) *n*-butylbenzene and *n*-heptanol, (b) *n*-butylbenzene and *n*-pentanol, (c) ethylbenzene and *n*-pentanol, (d) toluene and *n*-hexanol, (e) toluene and *n*-heptanol, and (f) *n*-propylbenzene and *n*-hexanol. The volume ratios of aromatic solvent to alcohol are set to 1:2 in all systems.

interface of C_{70}/TMB and *n*-heptanol. It is evident these morphologies are quite similar to the secondary units of the C_{70} hierarchical structures prepared from the corresponding solvents (Figure 2b2−d2). Moreover, the XRD patterns of **C70−TMB**, **C70−HA**, and **C70−TMB/HA** are cubic, monoclinic, and orthorhombic, which are consistent with those of **C70−P−TMB**, **C70−P−HA**, and **C70−P−TMB/HA**, respectively. Accordingly, we propose a formation mechanism for the C_{70} hierarchial structures, as demonstrated in Figure 1b. During the second step, when pure TMB or *n*-heptanol is used (Figure 1**bI**), C_{70} molecules from C_{70} microrods are dissolved in TMB or *n*-heptanol, and subsequently C_{70} nanocube-like units are formed after the evaporation of the solvents. Then the nanocubes gradually replace the original microrods as the process proceeds. In sharp contrast, when the mixed solvent (TMB/*n*-heptanol mixture) is applied (Figure 1bII), C_{70} molecules preferentially dissolve in TMB due to the higher solubility than that in *n*-heptanol.[38] Thus, the dissolved C_{70} molecules are localized in the cavity of the good solvent TMB, which is surrounded by *n*-heptanol, and the C_{70}/TMB/*n*-heptanol interfaces facilitate the C_{70} molecules to self-organize into C_{70} nanorods.[14] In this way, numerous nanorods are formed with the continuous dissolution of C_{70} microrods when the precipitation process proceeds, which finally facilitates the formation of the hierarchical structure consisting of nanorods. Interestingly, the solubility of C_{70} in TMB (1.45 mg/mL) or in *n*-heptanol (0.046 mg/mL) is too low to dissolve the C_{70} films thoroughly.[38] Accordingly, it should be a gradual progress that initially the surfaces and finally the cores of the C_{70} microrods participate in the reassembly process, which fundamentally facilitates the formation of the resultant hierarchical structures retaining the initial microrod-like morphology.

To verify the feasibility and versatility of this method, C_{70} hierarchical structures were prepared when various solvents were applied in the drop-drying process. As shown in Figure 6, echinacea-like morphologies are formed when *n*-butylbenzene/*n*-heptanol mixture is applied, while irregular microcubes are formed at surfaces when *n*-butylbenzene/*n*-pentanol mixture is used. However, when ethylbenzene/*n*-pentanol or toluene/*n*-hexanol mixture is employed, the C_{70} microrods evolve to C_{70} hierarchical structures composed of nanorods with different alignment at the surfaces for the two cases. Besides, as for the cases of toluene/*n*-heptanol and *n*-propylbenzene/*n*-hexanol, the final C_{70} hierarchical structures are built up with nanoparticles of different morphological features. It is obvious that the secondary structure varies upon the alteration of the employed solvent; thus, the morphology of the hierarchical structure can be easily controlled by proper solvent-choosing. Moreover, C_{60} hierarchical structures are obtained from the two-step self-assembly route (Figure S6) as well. Overall, the results discussed above indicate that our approach is a facile route for the fabrication of fullerene hierarchical structures, which is quite controllable and feasible.

It is widely acknowledged that, in the effort to artificially mimic water-repellent surfaces, a rough fractal interfacial morphology is necessary.[43] Moreover, thin films consisting of fullerenes or fullerene derivatives are reported to be hydrophobic surfaces.[28−30] Thus, the water contact angles are measured to observe how the hierarchical structures effect the hydrophobic properties of the as-prepared C_{70} films (Figure 7) and C_{60} films (Figure S7). As shown in Figure 7b, the mechanically pressed C_{70} film without the presence of ordered nano/microstructures (Figure 7a) is actually hydrophilic with a water angle of 66.55° ($\theta < 90°$). In sharp contrast, the thin films of C_{70} microrods and C_{70} hierarchical structures are all featured with hydrophobic properties, with the water contact angles of 142.75°, 145.90°, 147.29°, and 154.12° for **C70−P**, **C70−P−TMB**, **C70−P−HA**, and **C70−P−TMB/HA**, respectively. It is evident that hydrophobicity is markedly improved when C_{70} hierarchical structures are introduced, especially for **C70−P−TMB/HA** ($\theta > 150°$, superhydrophobic). Accordingly, the proper fabrication of hierarchical architectures can effectively help to improve the hydrophobicity of fullerene micro/nanostructures.

To further investigate the properties of the as-prepared fullerene hierarchical structures, their PL spectra were also measured, which leads to the finding of PL enhancement for the C_{70} hierarchical structures (Figure 8) and C_{60} hierarchical structures (Figure S8). The PL band positions for C_{70} powder, **C70−P**, and the corresponding C_{70} hierarchical structures are displayed in Table S2. The emission spectral changes such as red shift and peak broadening are obviously observed, similar to the C_{70} aggregates reported before.[14,44] Besides, significant PL enhancements are displayed for C_{70} hierarchical structures

DOI: 10.1021/acsami.5b05869
ACS Appl. Mater. Interfaces 2015, 7, 20285−20291

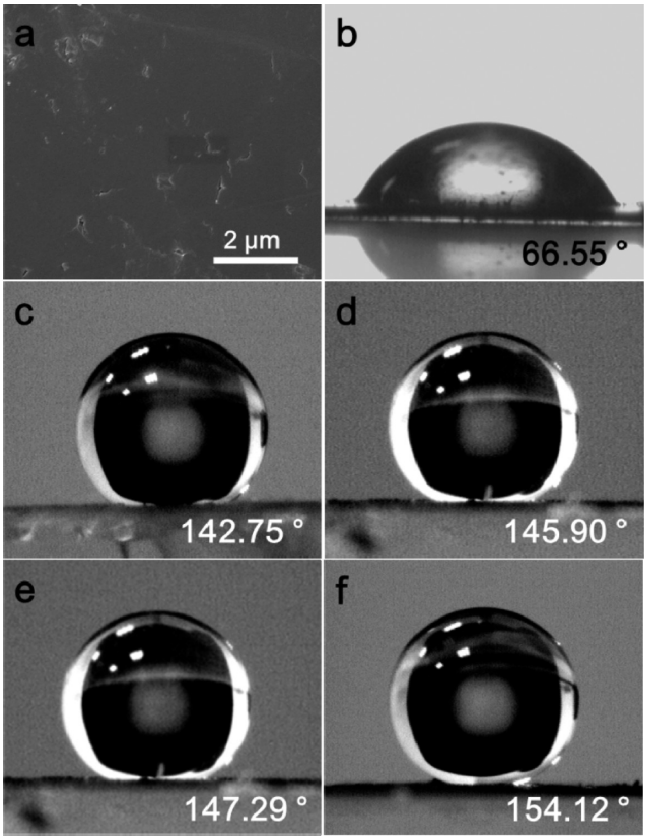

Figure 7. (a) SEM image of the mechanically pressed C_{70} film prepared from C_{70} powder, the photographs of a water droplet on the films of different C_{70} samples, (b) the mechanically pressed C_{70} film, (c) **C70−P**, (d) **C70−P−TMB**, (e) **C70−P−HA**, and (f) **C70−P−TMB/HA**.

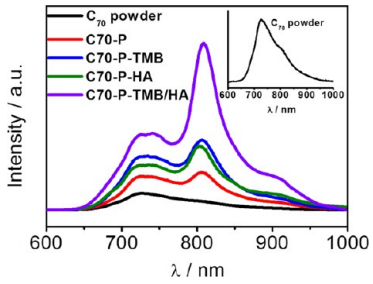

Figure 8. PL spectra for C_{70} powder, **C70−P**, **C70−P−TMB**, **C70−P−HA**, and **C70−P−TMB/HA**. The inset shows the magnified PL spectrum for C_{70} powder. PL spectra were recorded at room temperature upon excitation using a green laser at 514.5 nm.

when compared to C_{70} powder or the initial C_{70} microrods, especially for **C70−P−TMB/HA**. The PL spectra for C_{70} powder shows one prominent peak located at 726 nm with a 793 nm shoulder. However, the PL spectra of **C70−P** and the corresponding C_{70} hierarchical structures have the characteristic of two prominent peaks located at 730 and 805 nm, respectively. Surprisingly, **C70−P−TMB/HA** even has a dominant peak at 808 nm, displaying different PL features when compared to that of C_{70} powder. Since NMR and TGA results discussed above demonstrate that different solvents are incorporated in these C_{70} samples, we thus suppose that the interactions between the trapped solvents and C_{70} molecules are responsible for the PL enhancement.[45] Furthermore, the PL spectra of C_{70} hierarchical structures without the incorporation of solvent molecules (after high-temperature treatment) (Figure S9) and UV−vis−NIR spectra (Figure S10) are provided to illustrate the cause for the unique PL features. The PL enhancement of C_{70} hierarchical structures after desolvation is clearly displayed, demonstrating that the unique hierarchical morphologies are also responsible for the PL enhancement.[14] However, there is a sharp decrease of the PL intensity at the second peak of C_{70} hierarchical structures in comparison with the respective original samples, which provides clear evidence that the excited states and also the vibronic bands depend strongly on the trapped solvents.[46,47] Besides, the UV−vis−NIR spectra (Figure S10) of C_{70} microrods and C_{70} hierarchical structures are almost identical, which reveals that the trapped solvents affect the excited states but not the ground states of these samples. Accordingly, the unique PL behaviors of **C70−P−TMB/HA** are ascribed to the high content (17.52%) of solvent incorporation, with both TMB and *n*-heptanol trapped inside, and also the unique hierarchical morphology.

CONCLUSION

In summary, a two-step self-assembly method, which is quite simple and facile, is developed for the fabrication of fullerene hierarchical architectures. The key points for this method are that precipitation method is utilized to synthesize the initial fullerene microstructures, while the following drop-drying process is applied to reconstruct the initial fullerene microstructures into hierarchical structures. Furthermore, the solvents applied in the drop-drying process are incorporated into the C_{70} crystals, which consequently determine the second-level morphological features and crystalline types of the final products. With this method, different hierarchical structures are readily prepared simply by changing the solvents employed in the precipitation or the drop-drying process. Finally, the hierarchical structures exhibit hydrophobic properties, even superhydrophobicity, while the C_{70} film without the presence of nano/microstructure is hydrophilic. On the other hand, the C_{70} hierarchical structures all have enhanced photoluminescence behaviors in contrast with C_{70} powder, caused by the incorporation of solvent molecules in the C_{70} crystals and also the unique hierarchical architectures. Therefore, the universality and feasibility of this method make it a promising route to design fullerene hierarchical architectures of different molecular structures and diverse morphologies for the applications such as waterproof optoelectronic devices.

EXPERIMENTAL SECTION

Preparation of C_{70} Hierarchical Structures. In the first step, C_{70} microrods (**C70−P**) were synthesized following the aforementioned precipitation method,[37] and the concentration of C_{70} in *p*-xylene was 2.5 mg/mL. After centrifugation and vacuum drying of the precipitates, C_{70} microrods (4 mg) were collected and dispersed in isopropyl alcohol (IPA, 100 μL) to prepare a uniform suspension by ultrasounding for 10 min. Then a C_{70} film was formed by drop-casting the above suspension (2 μL) onto an ITO glass (5 mm × 5 mm) and left in vacuum oven (50 °C) for 2 h to completely dry off the IPA solvents from the samples. In the second assembly process, a small aliquot (2 μL) of desired solvent was dropped right onto the as-prepared C_{70} microrod film, using a pipet. After evaporation of the dropped solvents at 25 °C, the final C_{70} hierarchical structures were obtained. In our first attempt to fabricate C_{70} hierarchical structures, three kinds of solvents were employed in the drop-drying process: 1,3,5-trimethylbenzene (TMB), *n*-heptanol, and mixtures of TMB and

DOI: 10.1021/acsami.5b05869
ACS Appl. Mater. Interfaces 2015, 7, 20285−20291

n-heptanol ($v_{TMB}/v_{n\text{-heptanol}}$ = 1/2). The C_{70} hierarchical structures prepared from these three samples are designated as **C70−P−TMB**, **C70−P−HA**, and **C70−P−TMB/HA**, respectively. Furthermore, we also applied different solvents in the drop-drying process to verify the feasibility of our approach, such as the mixtures of *n*-butylbenzene and *n*-heptanol, *n*-butylbenzene and *n*-pentanol, toluene and *n*-heptanol, toluene and *n*-hexanol, ethylbenzene and *n*-pentanol, and *n*-propylebenzene and *n*-hexanol; the volume ratios of aromatic solvent to alcohol were set to 1:2 in all systems.

Control Experiments. In the attempts to investigate the formation mechanism of the hierarchical structures, one-step drop-drying or precipitation experiment was carried out. For the drop-drying process, saturated C_{70}/TMB or C_{70}/*n*-heptanol solution was applied. The saturated C_{70} solution (2 μL) was dropped onto ITO glasses (5 mm × 5 mm) by a pipet. Then the ITO glass with the saturated C_{70} solution inside was left still at 25 °C for drop-drying. The resulting products are denoted as **C70−TMB** and **C70−HA**, respectively. For the precipitation process, TMB was applied as the good solvent and *n*-heptanol as the antisolvent for C_{70}. Then C_{70} saturated solution in TMB (2 mL) was rapidly injected to *n*-heptanol (4 mL), the mixture was left still at room temperature for precipitation, and the product is designated as **C70-TMB/HA**. Furthermore, to study the structural transition of C_{70} hierarchical structures and the PL feature of the samples without the intercalation of solvent molecules, the three samples (**C70−P-TMB**, **C70−P−HA**, and **C70−P−TMB/HA**) were annealed at 400 °C for 2 h in Ar atmosphere to ensure the complete elimination of any intercalated solvents in the C_{70} crystals; the annealed samples are denoted as **C70−P−TMB−400**, **C70−P−HA−400**, and **C70−P−TMB/HA-400**, respectively.

Preparation of C_{60} Hierarchical Structures. C_{60} hexagonal prisms (**C60−O**) were initially prepared by a precipitation method using the solvent system of C_{60}/*o*-xylene/*n*-propanol (C_{60}/*o*-xylene: 2 mg/mL, 10 mL, *n*-propanol: 20 mL). After centrifugation and vacuum-drying process, C_{60} microstructures were dispersed in IPA at a concentration of 40 mg/mL. Then the C_{60} films were prepared and treated in the same way as that of C_{70} films. The solvents used for drop-drying process here were TMB/IPA (v/v = 1/2) mixture and CCl_4, with other conditions identical to those for the preparation of C_{70} hierarchical structures. The as-prepared C_{60} hierarchical structures are denoted as **C60−O−TMB/IPA** and **C60−O−CCl_4**, respectively. In addition, in the control experiments, the C_{60} nanorods (as shown in Figure S5) were prepared by the precipitation method using the solvent system of saturated C_{60}/TMB solution (2 mL) and IPA (4 mL).

Characterizations. The morphologies of all the products were examined by scanning electron microscopy (SEM, Nova NanoSEM 450) with an ultrathin Au coating. TEM images were collected by a Tecnai G2 F30 transmission electron microscope at 300 kV. X-ray diffraction patterns were obtained using an Empyrean diffractometer with Cu Kα radiation (λ = 0.1541 nm, operated at 40 kV and 40 mA). Raman scattering (Bruker VERTEX 70) samples were excited using a green laser at 514.5 nm and 0.05 mW power. FT-IR spectra were recorded on a Bruker Tensor-27 spectrometer. ^{1}H spectra were recorded at 600 MHz in $CDCl_3/CS_2$. Thermogravimetric analysis (TGA, Diamond TG/DTA) was performed to determine the solvent content in the final samples, and all the samples for TGA were dried in vacuum at 60 °C in prior. The measurements of the water contact angles were performed on a USA kino SL200. Photoluminescence spectra were obtained from a Bruker VERTEX 70 (samples were excited using a green laser at 514.5 nm with 0.05 mW power). UV−vis−NIR absorption spectra were obtained with a PE Lambda 750S spectrometer using the films composed of C_{70} micro/nanostructures on ITO glasses.

■ ASSOCIATED CONTENT

Supporting Information

The Supporting Information is available free of charge on the ACS Publications website at DOI: 10.1021/acsami.5b05869.

FTIR, Raman, DTG, ^{1}H NMR, and XRD results of C_{70} micro/nanostructures under study; the table showing the structural features of C_{70} microrods and C_{70} hierarchical structures. SEM images of C_{60} nanorods, the initial C_{60} hexagonal prisms, and C_{60} hierarchical structures, C_{60} mechanically pressed film; photographs obtained from water contact angle measurements and PL spectra of C_{60} mechanically pressed film, C_{60} hexagonal prisms, and C_{60} hierarchical structures; tables listing the photoluminescence band positions of C_{60} and C_{70} microstructures and their corresponding hierarchical structures. PL spectra of C_{70} hierarchical structures after high-temperature annealing and UV−vis−NIR absorption spectra of the films composed of C_{70} micro/nanostructures under study. (PDF)

■ AUTHOR INFORMATION

Corresponding Author

*Tel. and fax: (+86)27-87559404. E-mail: lux@hust.edu.cn.

Present Address

State Key Laboratory of Materials Processing and Die & Mold Technology, School of Materials Science and Engineering, Huazhong University of Science and Technology (HUST), Wuhan 430074, P. R. China.

Notes

The authors declare no competing financial interest.

■ ACKNOWLEDGMENTS

Financial support from The National Thousand Talents Program of China, NSFC (21171061, 51472095), Program for Changjiang Scholars and Innovative Research Team in University (IRT1014) and HUST is gratefully acknowledged. We thank the Analytical and Testing Center in Huazhong University of Science and Technology for all related measurements.

■ REFERENCES

(1) Thompson, B. C.; Fréchet, J. M. J. Polymer−Fullerene Composite Solar Cells. *Angew. Chem., Int. Ed.* **2008**, *47*, 58−77.

(2) Nakanishi, T. Supramolecular Soft and Hard Materials Based on Self-Assembly Algorithms of Alkyl-Conjugated Fullerenes. *Chem. Commun.* **2010**, *46*, 3425−3436.

(3) Babu, S. S.; Mohwald, H.; Nakanishi, T. Recent Progress in Morphology Control of Supramolecular Fullerene Assemblies and Its Applications. *Chem. Soc. Rev.* **2010**, *39*, 4021−4035.

(4) Hollamby, M. J.; Karny, M.; Bomans, P. H. H.; Sommerdjik, N.N. A. J. M.; Saeki, A.; Seki, S.; Minamikawa, H.; Grillo, I.; Pauw, B. R.; Brown, P.; Eastoe, J.; Möhwald, H.; Nakanishi, T. Directed Assembly of Optoelectronically Active Alkyl-π-Conjugated Molecules by Adding n-Alkanes or π-Conjugated Species. *Nat. Chem.* **2014**, *6*, 690−696.

(5) Zheng, S.; Ju, H.; Lu, X. A High-Performance Supercapacitor Based on KOH Activated 1D C_{70} Microstructures. *Adv. Energy Mater.* **2015**, *5*, 1500871.

(6) Li, H.; Tee, B. C. K.; Cha, J. J.; Cui, Y.; Chung, J. W.; Lee, S. Y.; Bao, Z. High-Mobility Field-Effect Transistors from Large-Area Solution-Grown Aligned C_{60} Single Crystals. *J. Am. Chem. Soc.* **2012**, *134*, 2760−2765.

(7) Saran, R.; Nordin, M. N.; Curry, R. J. Facile Fabrication of PbS Nanocrystal:C_{60} Fullerite Broadband Photodetectors with High Detectivity. *Adv. Funct. Mater.* **2013**, *23*, 4149−4155.

(8) Wei, L.; Yao, J.; Fu, H. Solvent-Assisted Self-Assembly of Fullerene into Single-Crystal Ultrathin Microribbons as Highly Sensitive UV-Visible Photodetectors. *ACS Nano* **2013**, *7*, 7573−7582.

DOI: 10.1021/acsami.5b05869
ACS Appl. Mater. Interfaces 2015, 7, 20285−20291

(9) Zhang, J.; Tan, J.; Ma, Z.; Xu, W.; Zhao, G.; Geng, H.; Di, C. a.; Hu, W.; Shuai, Z.; Singh, K.; Zhu, D. Fullerene/Sulfur-Bridged Annulene Cocrystals: Two-Dimensional Segregated Heterojunctions with Ambipolar Transport Properties and Photoresponsivity. *J. Am. Chem. Soc.* **2013**, *135*, 558−561.
(10) Minami, K.; Kasuya, Y.; Yamazaki, T.; Ji, Q.; Nakanishi, W.; Hill, J. P.; Sakai, H.; Ariga, K. Highly Ordered 1D Fullerene Crystals for Concurrent Control of Macroscopic Cellular Orientation and Differentiation toward Large-Scale Tissue Engineering. *Adv. Mater.* **2015**, *27*, 4020−4026.
(11) Mas-Torrent, M.; Rovira, C. Role of Molecular Order and Solid-State Structure in Organic Field-Effect Transistors. *Chem. Rev.* **2011**, *111*, 4833−4856.
(12) Su, B.; Wu, Y.; Jiang, L. The Art of Aligning One-Dimensional (1D) Nanostructures. *Chem. Soc. Rev.* **2012**, *41*, 7832−7856.
(13) Shrestha, L. K.; Yamauchi, Y.; Hill, J. P.; Miyazawa, K. i.; Ariga, K. Fullerene Crystals with Bimodal Pore Architectures Consisting of Macropores and Mesopores. *J. Am. Chem. Soc.* **2013**, *135*, 586−589.
(14) Park, C.; Yoon, E.; Kawano, M.; Joo, T.; Choi, H. C. Self-Crystallization of C_{70} Cubes and Remarkable Enhancement of Photoluminescence. *Angew. Chem., Int. Ed.* **2010**, *49*, 9670−9675.
(15) Wei, L.; Lei, Y.; Fu, H.; Yao, J. Fullerene Hollow Microspheres Prepared by Bubble-Templates as Sensitive and Selective Electrocatalytic Sensor for Biomolecules. *ACS Appl. Mater. Interfaces* **2012**, *4*, 1594−1600.
(16) Shin, H. S.; Yoon, S. M.; Tang, Q.; Chon, B.; Joo, T.; Choi, H. C. Highly Selective Synthesis of C_{60} Disks on Graphite Substrate by a Vapor−Solid Process. *Angew. Chem., Int. Ed.* **2008**, *47*, 693−696.
(17) Zhang, E.-Y.; Wang, C.-R. Fullerene Self-Assembly and Supramolecular Nanostructures. *Curr. Opin. Colloid Interface Sci.* **2009**, *14*, 148−156.
(18) Park, C.; Song, H. J.; Choi, H. C. The Critical Effect of Solvent Geometry on the Determination of Fullerene (C_{60}) Self-Assembly into Dot, Wire, and Disk Structures. *Chem. Commun.* **2009**, 4803−4805.
(19) Kim, J.; Park, C.; Park, J. E.; Chu, K.; Choi, H. C. Vertical Crystallization of C_{60} Nanowires by Solvent Vapor Annealing Process. *ACS Nano* **2013**, *7*, 9122−9128.
(20) Breuer, T.; Witte, G. Diffusion-Controlled Growth of Molecular Heterostructures: Fabrication of Two-, One-, and Zero-Dimensional C_{60} Nanostructures on Pentacene Substrates. *ACS Appl. Mater. Interfaces* **2013**, *5*, 9740−9745.
(21) Chen, X.; Mao, S. S. Titanium Dioxide Nanomaterials: Synthesis, Properties, Modifications, and Applications. *Chem. Rev.* **2007**, *107*, 2891−2959.
(22) Nikoobakht, B.; Wang, X.; Herzing, A.; Shi, J. Scalable Synthesis and Device Integration of Self-Registered One-Dimensional Zinc Oxide Nanostructures and Related Materials. *Chem. Soc. Rev.* **2013**, *42*, 342−365.
(23) Magasinski, A.; Dixon, P.; Hertzberg, B.; Kvit, A.; Ayala, J.; Yushin, G. High-Performance Lithium-Ion Anodes Using a Hierarchical Bottom-Up Approach. *Nat. Mater.* **2010**, *9*, 353−358.
(24) Wu, J.-J.; Liao, W.-P.; Yoshimura, M. Soft Processing of Hierarchical Oxide Nanostructures for Dye-Sensitized Solar Cell Applications. *Nano Energy* **2013**, *2*, 1354−1372.
(25) Gao, X.; Jiang, L. Biophysics: Water-Repellent Legs of Water Striders. *Nature* **2004**, *432*, 36−36.
(26) Li, Y.; Dai, S.; John, J.; Carter, K. R. Superhydrophobic Surfaces from Hierarchically Structured Wrinkled Polymers. *ACS Appl. Mater. Interfaces* **2013**, *5*, 11066−11073.
(27) Amer, M. S.; Busbee, J. D. Self-Assembled Hierarchical Structure of Fullerene Building Blocks; Single-Walled Carbon Nanotubes and C_{60}. *J. Phys. Chem. C* **2011**, *115*, 10483−10488.
(28) Nakanishi, T.; Michinobu, T.; Yoshida, K.; Shirahata, N.; Ariga, K.; Möhwald, H.; Kurth, D. G. Nanocarbon Superhydrophobic Surfaces Created from Fullerene-Based Hierarchical Supramolecular Assemblies. *Adv. Mater.* **2008**, *20*, 443−446.
(29) Zhang, X.; Takeuchi, M. Controlled Fabrication of Fullerene C_{60} into Microspheres of Nanoplates through Porphyrin-Polymer-Assisted Self-Assembly. *Angew. Chem., Int. Ed.* **2009**, *48*, 9646−9651.
(30) Nakanishi, T.; Shen, Y.; Wang, J.; Li, H.; Fernandes, P.; Yoshida, K.; Yagai, S.; Takeuchi, M.; Ariga, K.; Kurth, D. G.; Mohwald, H. Superstructures and Superhydrophobic Property in Hierarchical Organized Architectures of Fullerenes Bearing Long Alkyl Tails. *J. Mater. Chem.* **2010**, *20*, 1253−1260.
(31) Sathish, M.; Miyazawa, K. i. Size-Tunable Hexagonal Fullerene (C_{60}) Nanosheets at the Liquid-Liquid Interface. *J. Am. Chem. Soc.* **2007**, *129*, 13816−13817.
(32) Ji, H.-X.; Hu, J.-S.; Tang, Q.-X.; Song, W.-G.; Wang, C.-R.; Hu, W.-P.; Wan, L.-J.; Lee, S.-T. Controllable Preparation of Submicrometer Single-Crystal C_{60} Rods and Tubes Trough Concentration Depletion at the Surfaces of Seeds. *J. Phys. Chem. C* **2007**, *111*, 10498−10502.
(33) Shrestha, R. G.; Shrestha, L. K.; Khan, A. H.; Kumar, G. S.; Acharya, S.; Ariga, K. Demonstration of Ultrarapid Interfacial Formation of 1D Fullerene Nanorods with Photovoltaic Properties. *ACS Appl. Mater. Interfaces* **2014**, *6*, 15597−15603.
(34) Amer, M. S.; Todd, T. K.; Busbee, J. D. Effect of Linear Alcohol Molecular Size on the Self-Assembly of Fullerene Whiskers. *Mater. Chem. Phys.* **2011**, *130*, 90−94.
(35) Yao, M.; Fan, X.; Liu, D.; Liu, B.; Wågberg, T. Synthesis of Differently Shaped C_{70} Nano/Microcrystals by Using Various Aromatic Solvents and Their Crystallinity-Dependent Photoluminescence. *Carbon* **2012**, *50*, 209−215.
(36) Geng, J.; Zhou, W.; Skelton, P.; Yue, W.; Kinloch, I. A.; Windle, A. H.; Johnson, B. F. G. Crystal Structure and Growth Mechanism of Unusually Long Fullerene (C_{60}) Nanowires. *J. Am. Chem. Soc.* **2008**, *130*, 2527−2534.
(37) Zheng, S.; Lu, X. Formation Kinetics and Photoelectrochemical Properties of Crystalline C_{70} One-Dimensional Microstructures. *RSC Adv.* **2015**, *5*, 38202−38208.
(38) Semenov, K. N.; Charykov, N. A.; Keskinov, V. A.; Piartman, A. K.; Blokhin, A. A.; Kopyrin, A. A. Solubility of Light Fullerenes in Organic Solvents. *J. Chem. Eng. Data* **2010**, *55*, 13−36.
(39) Schettino, V.; Pagliai, M.; Cardini, G. The Infrared and Raman Spectra of Fullerene C_{70}. DFT Calculations and Correlation with C_{60}. *J. Phys. Chem. A* **2002**, *106*, 1815−1823.
(40) Ghosh, G.; Sastry, V.; Sundar, C.; Radhakrishnan, T. Structural Transformation in HCP Solid C_{70} at Low Temperatures. *Solid State Commun.* **1998**, *105*, 247−251.
(41) Isakina, A. P.; Prokhvatilov, A. I.; Strzhemechny, M. A.; Yagotintsev, K. A. Structure, Lattice Parameters, and Thermal Expansion Anisotropy of C_{70} Fullerite. *Low Temp. Phys.* **2001**, *27*, 1037−1047.
(42) Takahashi, Y. Structural Model of Toluene-Solvated C_{70} from High-Resolution Transmission Electron Microscopy. *Chem. Phys. Lett.* **1998**, *292*, 547−553.
(43) Sun, T.; Feng, L.; Gao, X.; Jiang, L. Bioinspired Surfaces with Special Wettability. *Acc. Chem. Res.* **2005**, *38*, 644−652.
(44) Ichida, M.; Sakai, M.; Yajima, T.; Nakamura, A.; Shinohara, H. Luminescence Due to Intra- and Inter-Molecular Transition in C_{70} Single Crystals. *Chem. Phys. Lett.* **1997**, *271*, 27−32.
(45) Martins, S.; Fedorov, A.; Afonso, C. A. M.; Baleizão, C.; Berberan-Santos, M. N. Fluorescence of Fullerene C_{70} in Ionic Liquids. *Chem. Phys. Lett.* **2010**, *497*, 43−47.
(46) Warntjes, J. B. M.; Holleman, I.; Meijer, G.; Groenen, E. J. J. Photoluminescence of Molecular C_{70} at 1.5 K. On the Nature of the Lowest Excited States. *Chem. Phys. Lett.* **1996**, *261*, 495−501.
(47) Argentine, S. M.; Kotz, K. T.; Francis, A. H. Temperature and Solvent Effects on the Luminescence Spectrum of C_{70}: Assignment of the Lowest Singlet and Triplet States. *J. Am. Chem. Soc.* **1995**, *117*, 11762−11767.

DOI: 10.1021/acsami.5b05869
ACS Appl. Mater. Interfaces 2015, 7, 20285−20291